A THEORETICAL ALGORITHM FOR FEA ANALYSIS AND NC MANUFACTURING

MIHALACHE Marius[1] Andrei and NAGIT Gheorghe[1]

ABSTRACT: In the present study the authors propose a new algorithm for identifying the loads that act upon a functional connecting rod during a full engine cycle. The whole study relies on a theoretical mechanical project which was developed in order to identify the right values that correspond to each degree of the entire engine cycle of a Daewoo Tico automobile. On the basis of the obtained results the study then presents a sequence of operations performed in a 3D environment in order to obtain a full physical replica of a previously optimized 3D geometry of a connecting rod by means of NC driven manufacturing process. The connecting rod's 3D geometry was divided in two sections and considered individually as its head and body. Only important operations are presented in the study and the overall results.
KEY WORDS: FEA, 3D setup, connecting rod, CNC.

1 INTRODUCTION

In order to highlight the full behaviour of a part under certain loads, one should consider the entire working cycle of that part under all known loads that act upon it. This is a tedious work in case of all 720^{o} degrees of an engine cycle. The present is structured as a case study as it is developed solely for the Daewoo Tico's type of engine. Considering that previous studies showed that the behaviour of the connecting rods are different depending on the type of loads considered to act upon them, this leads to a significant amount of work and data's to be processed (Kim et al., 2015). Ours proposal is an algorithm which will identify only the values corresponding to engine cycle angles that produce a significant change; values that will override the ones that do not (Bagherpour et al., 2015). The considered load values are theoretical and have been produced by means of a technical project of a similar engine design. The resulted values were compared to similar ones presented by other researches in their studies which were found to be appropriate (Swaminathan et al., 2015).

On the other hand, the NC driven machining of single parts or components is an up to date technology, widely used throughout the entire mechanical related industries. Thus 3D environments that assist the engineers have developed special custom fitted modules to smooth the transition from a virtual geometry to a physical replica of it.

[1]"Gheorghe Asachi" Technical University of Iasi, Department of Machine Manufacturing Technology, Blvd. D. Mangeron, No. 59A, Iasi-700050, Romania E-mail:andrei.mihalache@yahoo.com; nagit@tcm.tuiasi.ro

In the present study, the authors are using *Catia* in order to generate the sequence of operations needed for the *Mazak Nexus 510C* NC centre to manufacture a connecting rod. The parts have undergone a series of tests that provided the authors with an optimization procedure and the corresponding geometry (Swaminathan et al., 2015). A few print screens of simulated operations performed on the geometry are provided. The connecting rod's geometry was considered intricate enough because it contains lots of free form surfaces, angles, transition zones, inner channels or fillets that without a powerful 3D tool as *Catia* or something similar would be very hard if not impossible to machine by means of NC manufacturing which may prove someday to be a viable alternative to the classical forging process (Bagherpour et al., 2015).

2 METHOD DESCRIPTION

The loads that act upon the moving connecting rod are presented for two regimes: the *semi-dynamic* one and *dynamic* regime. The distribution of loads produces different results as it acts upon the connecting rod's head and body.

In case of the *semi-dynamic* regime we will take into account that the load that acts upon the connecting rod is an inertia type of force which breaks down into two components: axial and normal. The axial component is also divided into the tensile and compressive type of forces. This type of load regime is different from a static regime because it is considering the alternation of forces during an entire engine cycle and not at a given point in time as a static regime would. Considering each individual value corresponding to every angle out of the 720 ones would be time consuming and

very unproductive as we will demonstrate that certain critical values produce the same results. It is well known that the loads that act upon a certain point from within the connecting rod whole geometric surface have two major components: a bending and an axial form (Figure 1), (Bagherpour et al., 2015).

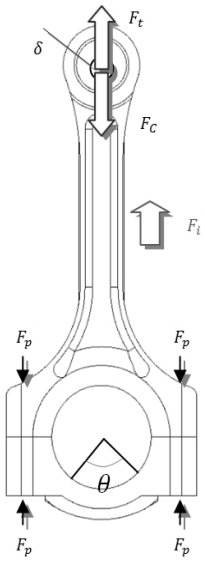

Figure. 1. Axial loads distribution on connecting rod's body.

The bending load depends on the bending momentum and it is expressed as a function of the load normal to the part's weight centre axis related to both angular and linear acceleration corresponding values. The variation of these loads during a half engine cycle from 0^o to 360^o is almost the same as the one from 360^o to 720^o. The F_i symbol from figure 1 represents the inertia type of force distributed on the entire surface of the connecting rod.

As presented above, the values of the axial loads on each end of the connecting rod are not identical at any time due to different inertia loads. This makes it equal in terms of deciding which end of the connecting rod to choose since axial components distribution is the same at both ends. In the present study, the authors applied the load to the connecting rod's body or the piston end of it (Figure 1). Results from the first half of an engine cycle had to be compared with the ones obtained from the other half. We have therefore overlapped the distributions under axial load characteristic to the first half of engine cycle with the one from the second half. Then we have divided these distributions into three different regions: "*i"*, "*ii"* and "*iii"*. Each segment of curve from each region received a letter from "*a"* to "*f"*. By comparing those segments we have been able to choose the ones which showed different variations and eliminate the ones which were overlapping (Figure 2).

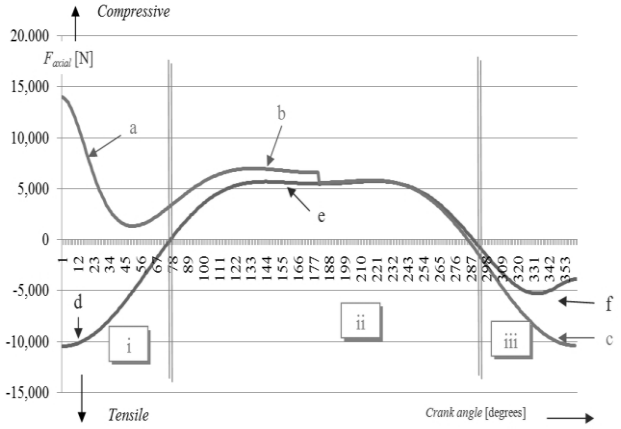

Figure. 2. Axial load distribution from 0^o to 360^o overlapped with the one from 360^o to 720^o.

The "*i"* region has two segments: "*a*" and "*d*". Both display different variations and do not overlap at any time.

The "*ii"* region has two segments: "*b*" and "*e*". The "*b*" segment shows a bigger variation in the compressive domain than "*e*" does up to 180^o then both being almost identical which led to the conclusion that segment "*e*" may be eliminated from the process. The lowest value from the variation of segment "*e*" was considered and then compared with the lowest one from segment "*b*" in order to validate the decision.

The "*iii"* region has also two segments: "*c*" and "*f*". Since segment "*c*" displays a bigger variation in the tensile domain than segment "*f*" does, the last one was eliminated. The lowest value from the variation of segment "*f*" was considered and then compared with the lowest one from segment "*c*" in order to validate the decision.

In order to highlight the behaviour of the connecting rod on a full engine cycle our method states that it is enough to consider only the segments "*a*", "*b*", "*c*" and "*d*". Since the first change of sign is being recorded for the 76^o angle the "*d*" segment will extend from 0^o to 75^o. In the same manner "*e*" will extend from 76^o to 287^o being divided around the 180^o angle. The "*f*" segment will extend from 288^o to 360^o. Region "*a*" will extend from 361^o to 435^o. Region "*b*" segment will extend from 436^o to 647^o being divided around the 540^o angle. In the end, region "*c*" will extend from 648^o to 720^o.

The critical values which will be considered in the evaluation process of the connecting rod on a full engine cycle are corresponding to the following

angles: 0°, 76°, 361°, 410°, 495°, 578°, 646° and 720°. In addition to those, values that are corresponding to the 220° and 332° angles from segments "*e*" and "*f*" were also considered in order to validate the method. The resulted distribution is presented in Figure 3.

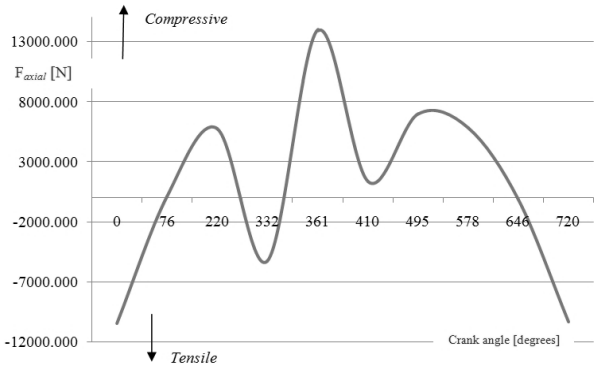

Figure. 3. Axial load distribution at proposed

The two main loads which were considered in the case of the *dynamic* regime are the tensile and the compressive ones. We have considered the assembly which consists of the connecting rod, the piston and the crank (Figure 4). The setup was developed in order to simulate as much as possible the real environment in which the process takes place. Thus it performs as it should under an inertia type of load.

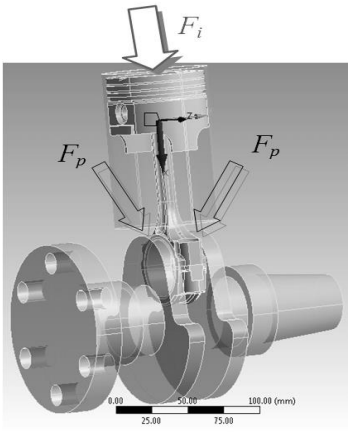

Figure. 4. The assembly: the connecting rod, the piston and the crank.

The difference from a *semi-dynamic* regime consists in the type of load that has to be applied to the piston's head in order to generate the motion of the considered assembly. This load considers the normal component of the inertia type of force thus making it suitable for a full dynamic FEA simulation (Kim et al., 2015). The inertia force or the total force as it is also known results from summing up the forces that appear due to the accumulated pressure of gases inside the cylinder, the translation inertia forces of moving masses, weight related forces and friction related forces. The distribution under inertia load over the first half of the engine cycle has been overlapped with the one from the second half. Then we have divided these distributions into three different regions: "*i*", "*ii*" and "*iii*". Each segment of curve from each region received a letter from "*a*" to "*f*" naming particular areas (Figure 5).

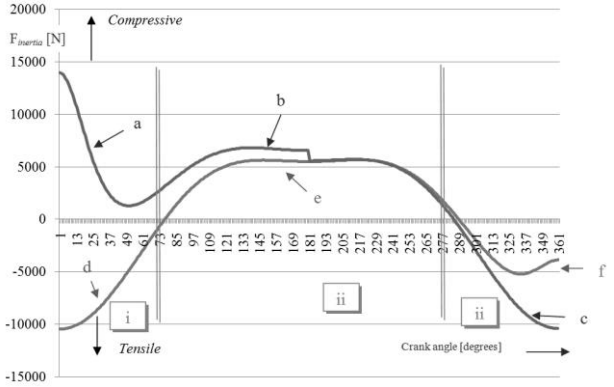

Figure. 5. Inertia load distribution from 0° to 360° overlapped with the one from 360° to 720°.

The "*i*" region has two segments: "*a*" and "*d*". Both display different variations and do not overlap at any time.

The "*ii*" region has two segments: "*b*" and "*e*". The "*b*" segment shows a bigger variation in the compressive domain than "*e*" does up to 180° then both being almost identical which led to the conclusion that segment "*e*" may be eliminated from the process. The lowest value from the variation of segment "*e*" was considered and then compared with the lowest one from segment "*b*" in order to validate the decision.

The "*iii*" region has also two segments: "*c*" and "*f*". Since segment "*c*" displays a bigger variation in the tensile domain than segment "*f*" does, the last one was eliminated. The lowest value from the variation of segment "*f*" was considered and then compared with the lowest one from segment "*c*" in order to validate the decision.

In order to highlight the behaviour of the assembly on a full engine cycle it is enough to consider only the segments "*a*", "*b*", "*c*" and "*d*". Since the first change of sign is being recorded for the 76° angle the "*d*" segment will extend from 0° to 75°. In the same manner "*e*" will extend from 76° to 287° being divided around the 180° angle. The "*f*" segment will extend from 288° to 360°. Region "*a*" will extend from 361° to 435°. The "*b*" segment will extend from 436° to 647° being divided around the

540° angle. In the end, "*c*" will extend from 648° to 720°.

The critical values which will be considered in the evaluation process of the connecting rod on a full engine cycle are corresponding to the following angles: 0°, 76°, 361°, 410°, 499°, 574°, 646° and 720°. In addition to those, values that are corresponding to the 215° and 333° angles from segments "*e*" and "*f*" were also considered in order to validate the method. The resulted distribution is presented in Figure 6.

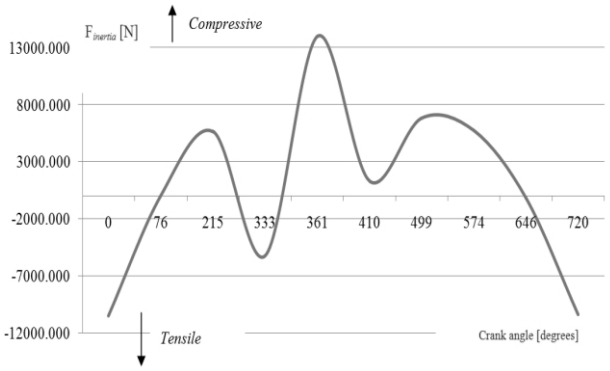

Figure. 6. Inertia load distribution at given critical angles.

Now that we have the entire behaviour of the connecting rod mapped for the engine cycle we have developed a method of FEA based analyses which led us to an optimized form of the original parts. The optimization is based on a weight loss on a certain area of the body as the theoretical results showed a better performance under given loads then the original. In the present analysis three steps have been considered: *the setup, the program* and *the output*. The setup involves analysing the part to be machined, choose the actual setup, define the geometry, define the collision zones and create the tools. Programming defines the operations that will actually machine the desired part. The output refers to the installation of the post processor which has to match the actual NC centre. Post processing converts the generic internal tool path data into a format which is compatible with a specific machine tool controller combination. In order to post process the user will need a tool path and the post processor itself.

2.1 Step 1: The setup.

The two components are digitized in form of *Catia* related files. By default the software imposes the alignment of parts to a unique coordinate system. The next step consisted on the definition of the blank as well as the part's geometry.

Next, we had to set a so called container or a collision free zone. Collision zones allow the cutter to avoid objects by using an axial containment plane (1), start and return points (2), and also a clearance plane (3), (Figure 7).

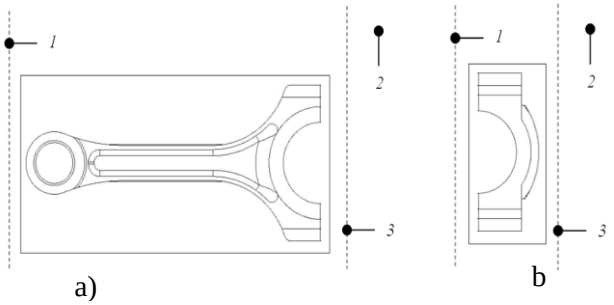

Figure 7. Collision zones setup.

a) The body of the connecting rod,

Another important step is to set up an avoidance perimeter in such a way to avoid a chuck in terms of the containment plane mentioned above. Operations such as roughing and finishing will need to use this containment group. Last step setups up the tools that will be used in the manufacturing process. In both cases we have defined different tools such as: face mills (*customized to meet the requirements of a cylindrical frontal type of mill*) with different diameters, cylindrical frontal mills with inclined tips, ball tip mills with different diameters. Fillet mills were substituted by the ball tip mills.

2.2 Step 2: The program.

In order to completely machine the connecting rod's head we had to set up seven different operations involving seven tool changes (Figure 8).

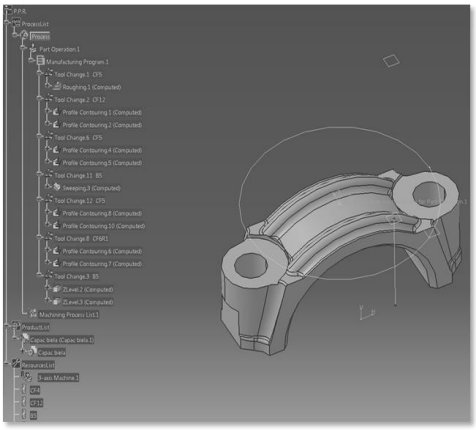

Figure 8. List of processes and

Some of the operations needed for the process of machining the desired part are: *roughing, profile contouring, sweeping* and *Z levelling*. Having defined a rough stock (*the blank from which the cutter will machine the desired part*), we have to "*tell*" the software where a safety plan (*the above mentioned containment plane*) begins and also

where the separation plane (*the above mentioned clearance plane*) does the same (Figure 9).

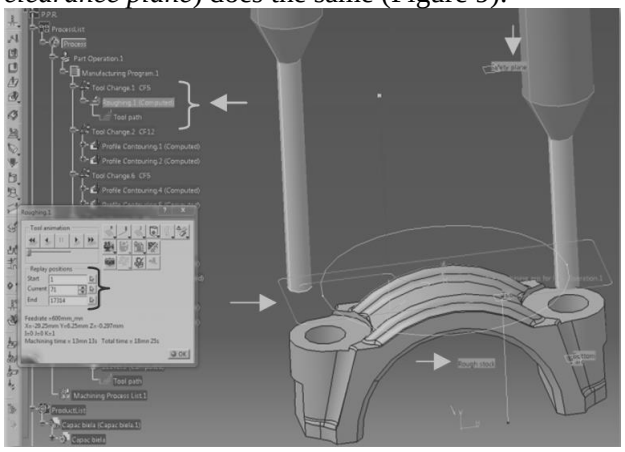

Figure 9. Defining the safety plane for the roughing operation.

This will be set apart from the outer upper diameter of the part's ribs. This makes the software to automatically show the cutter's position and alignment in with respect to the two defined planes as well as all the intermediate planes that the tool has to keep count of, in order to fully machine the imposed geometry (Figure 10).

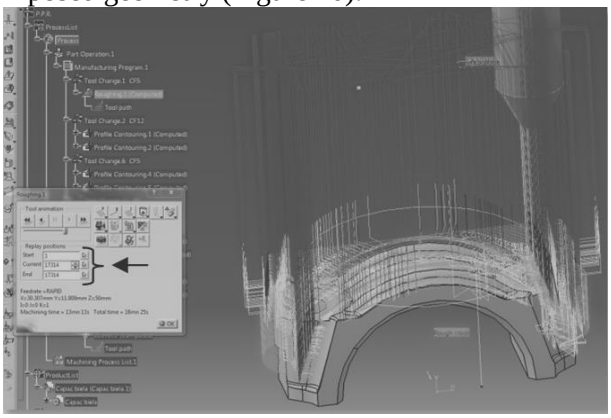

Figure 10. Roughing the connecting rod's head.

The tool that performs the roughing operation is a cylindrical frontal type of mill with a diameter of 5 mm (*CF5*).

Another operation required in order to properly machine the connecting rod's head is the *profile contouring*. It has been carried out in different steps with various tools such as cylindrical frontal mills with diameters of 12 and 5 mm (*CF12* and *CF5*) and also a cylindrical frontal mill with a diameter of 6 mm and its tip inclined by a radius of 1 mm (*CF6R1*). For now they have been machined at a given angle as afterwards they will need additional operations such as *Z* levelling. The holes for the bolts were profile contoured with the frontal cylindrical mill with its tip inclined after sweeping has taken place. Another operation is being represented by *sweeping*. It has been carried out with a ball tip mill with a diameter of 5 mm (B5). The operation is similar to finishing. It has been applied to the entire upper area of the connecting rod's head as it may be seen from Figure 11.

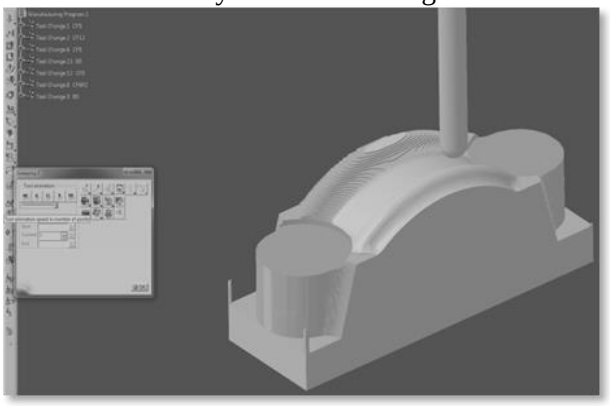

Figure 11. Sweeping the upper area of the connecting rod's head.

The last one of the operations needed in order to fully machine the connecting rod's head is represented by so called *Z levelling*. It is an operation carried out along the *Z* axis, which is also the tool axis. We can see that after a profile contouring we have an angled surface that wraps around the outer ring. This gets smooth out by *Z* levelling as we can observe from Figure 12.

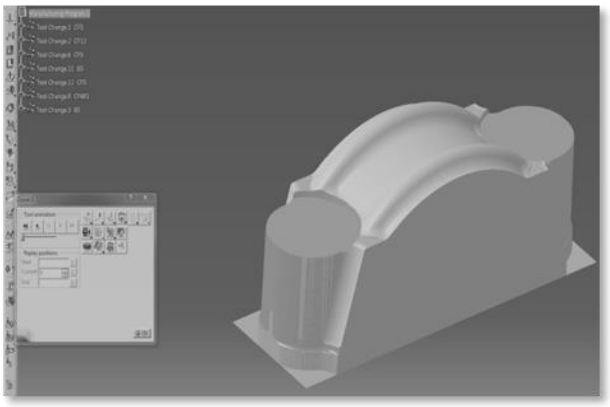

Figure 12. *Z* leveling transition zones of the connecting rod's head.

The operation substitutes a different change of tool, namely a fillet mill, needed for those specific areas.

In order to completely machine the connecting rod's body, we had to set up five different operations involving five tool changes. We started with a profile contouring operation designed to machine the holes that allow connections with the piston and the crank shaft performed with a cylindrical frontal mill of 6 mm (CF6). Then we had

to set up a roughing operation with the same type of tool (Figure 13).

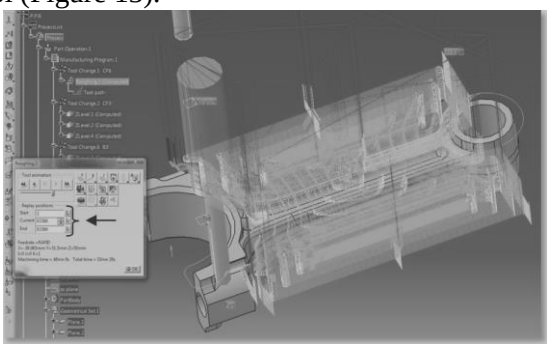

Figure 13. Roughing the connecting rod's bodv.

We can see all the intermediate planes that the tool has to take into account. They are directly related with the number of passes that the cutter has to make in order to complete the machining operation. Most of the connecting rod's body geometry will be covered in terms of machining by multiple *Z* levelling operations, more exact one for each end of the connecting rod's body and one for the inner channels. Special attention was given to the outer ribs which required precision and a small tool of less than 3 mm in diameter (CF2.95). The cutter moves from one end to another in such a way that it will also give contour to the inner channel. For the part's each end we needed a different set of *Z* levelling operations. As stated before even though the inner channels were partially machined due to the number of passes that the cutter had to perform, the precision part of the process is carried out with a ball tip mill of 3 mm (B3) in a distinctive operation specially designed for those areas (Figure 14).

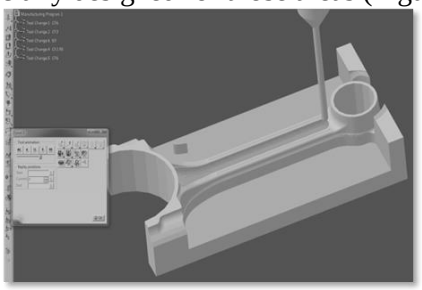

Figure 14. *Z* leveling the inner channels of the connecting rod's body.

2.3 Step 3: The output.

It refers to the definition and setup of post processing operations which will lead to the generation of the desired *G* code depending upon the NC centre's parameters and capabilities. The *Mazak Nexus 510C* is a single column, bed-type machine with 3 axes. It has its own postprocessor custom built which may be loaded to the software's database. The controller was fed to *Catia* under *Part Operations* menu (Figure 15).

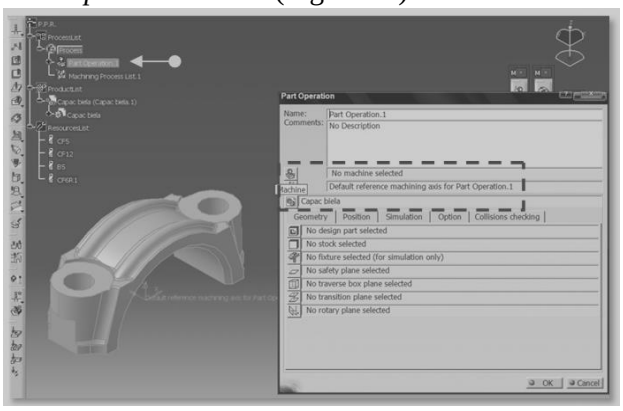

Figure 15. *Part Operation* menu for the connecting rod's head.

This "*tells*" the software that it should use as its post processor the file named "*mazak.lib*" which is in fact a library that contains all required parameters that are characteristic to the NC machine.

The equipment was set to a three axis machine which corresponds to the capabilities of the *Mazak Nexus 510C* centre (Figure 16).

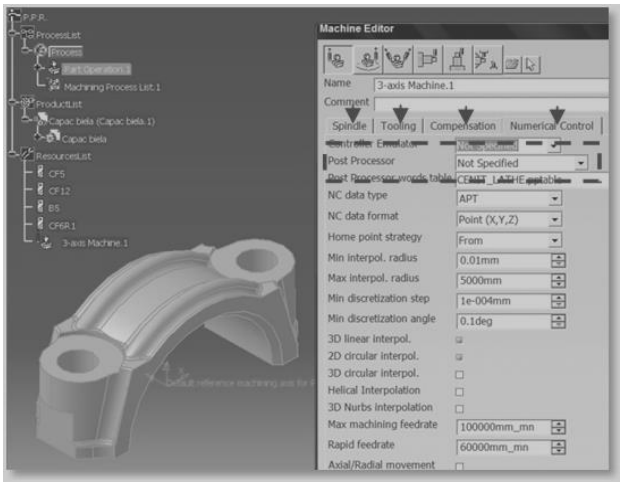

Figure 16. *Post Processor* definition menu for the connecting rod's head.

Under *Numerical Control* menu we have set proper values for *Spindle, Tooling* and *Compensation*. Under *Resulting NC Data* menu we have specified NC code and the location for the export files. It generated a total of 25 files for both of the connecting rod's components (Figure 17).

Part of a file which was exported with the *G code* command lines is presented for exemplification in table 1.

3 CONCLUSIONS

The proposed method applies to the regimes that stretch over an entire engine cycle. It identifies the values considered as critical that simulate the behaviour of the connecting rod just as if we would had to consider the all 720 of them that are corresponding to the angles from a full engine cycle.

In order to perform FEA analyses, constraints and loads should be set from the beginning. In the case of both *semi-dynamic* and *dynamic* regimes the

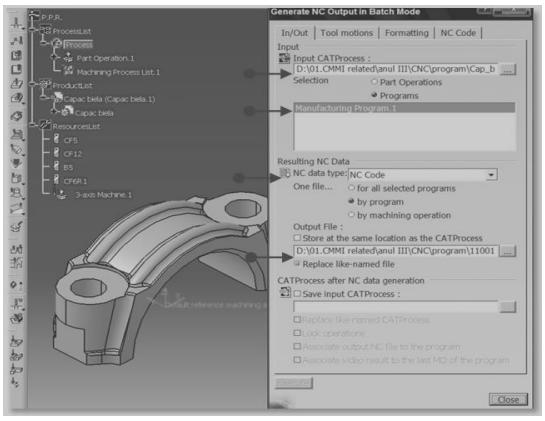

Figure 17. *G type NC Code* generation for the connecting rod's head.

Table 1. *G code* command lines fed to the NC centre.

Parameters	Command lines
:11001 N1 G90 G94 G64 G80 G40 G49 (CF5) N2 G91 G28 Z0 N3 G28 Y0 N4 G90 G54 N5 TxxTxx M6 N6 S8500 M3 X-14.648 Y-16.6 F5500 G43 Z70. Hxx M8	Z9.703 G1 Z-.297 M08 F1500. Y-11. X31. X32. F600. G3 X33. Y-10. R1. G1 Y-9. Y9. F1500. Y10. F600. G3 X32. Y11. R1. G1 X31.

method proves that in the case of FEA analysis considering only 8 critical values and two more for confirmation out of 720 would provide the user with the same perspective over the connecting rod's behaviour under given loads. The method may be extended to other types of working cycles as well not to mention all forms of connecting rods.

This paper also highlights some of the technical issues that can interfere in the transition procedure between a CAD environments displaying a 3D model to a NC command centre by means of which we may obtain a corresponding physical replica through NC driven machining technology.

The authors have presented workflow related steps in terms of setup, parameters or required functions. In case of the connecting rod's head we have defined seven operations which involved every time that tools had to be changed in order for the proper machining operation to take place. The most sensitive areas were the transition between fillets and inner surfaces as well as the ones that surround the outer rings with inner holes that are destined for bolts.

The best fitted function for this type of geometry is considered to be the *Z* levelling as it is capable of not only machine the specified areas but also smooth out the entire surface. In case of the connecting rod's body the same function was chosen in order to deal with sensitive areas such as the filleted transition zones at both piston and crank end of the part but also the inner channels, not to mention the outer fine ribs which stretch along the entire part's length. Not only that we have obtained a physical model but, in terms of costs and time, we have reduced greatly the amount that would have been required in order to perform an optimization procedure and then translate it into reality.

4 REFERENCES

►Swaminathan, K., *et al*. (2015). *Stress, vibration and buckling analyses of FGM plates—A state-of-the-art review*, available at: http://www.sciencedirect.com/science/article/pii/S0263822314005182, Accessed: 2016-04-22

►Bagherpour, E., *et al*. (2015). *An analytical approach for simple shear extrusion process with a linear die profile*, available at: http://www.sciencedirect.com/science/article/pii/S0264127515003731, Accessed: 2016-03-07

►Kim, J. G., *et al*. (2015). *Finite element analysis of the plastic deformation in tandem process of simple shear extrusion and twist extrusion*, available at: http://www.sciencedirect.com/science/article/pii/S0264127515003846, Accessed: 2016-03-17